SYNTHESIS OF ACOUSTIC-SURFACE-WAVE-RESONATOR FILTERS USING ANY OF VARIOUS COUPLING MECHANISMS†

G. L. Matthaei, E. B. Savage, and F. Barman
Electrical Engineering and Computer Science
University of California
Santa Barbara, California 93106

Abstract

Simple, flexible means are presented for synthesis of acoustic-surface-wave-resonator band-pass filters from low-pass prototypes. Methods for filters using resonators coupled by transducers, reflecting arrays, and multi-strip couplers are treated.

Introduction

It is well known that surface-wave resonators of the Fabry-Perot type can be fabricated using reflectors consisting of large arrays of reflecting elements.[1,2,3] Figure 1(a) illustrates one type of resonator which consists of arrays of metal strips (extending into and out of the paper) on the surface of a piezoelectric substrate such as $LiNbO_3$ or quartz. At resonance the arrays on the left and right act like reflecting walls for the surface-wave energy. Such resonators can be modelled quite well by a transmission-line equivalent circuit model as shown in Fig. 1(b). Note that the arrays are represented by a cascade of equal-length line sections with impedance Z_e alternating with Z_0. (We are free to set $Z_0 = 1/Y_0 = 1$ for convenience.) It has been found that for the small values of $r = Z_e/Z_0$ which are typical for SAW arrays, equal-line-length modelling of the arrays is a good approximation even if w and g are quite unequal in Fig. 1(a), provided appropriate values of wave velocity and r are used.[4]

Working from equivalent circuits such as that in Fig. 1(b) to represent the resonators, it is shown herein that known techniques used for microwave-filter design can be adapted for straight-forward design of surface-wave-resonator filters with any of a variety of different coupling mechanisms. Types of couplings to be treated are electrical couplings through transducers, acoustic coupling through reflecting arrays, and multistrip couplings.

Band-pass Parameters from Low-pass Prototypes

In Fig. 2(a) is shown a low-pass prototype filter of a type for which tabulated element values are available for Chebyshev, maximally flat, and other types.[5] In Fig. 2(b) is shown a possible form of band-pass filter which can be derived from the low-pass filter in Fig. 2(a). The boxes marked $J_{j,j+1}$ are "admittance inverters" which operate at all frequencies like a quarter-wavelength section of transmission line having characteristic admittance $J_{j,j+1}$. Note that a parallel-type resonator in shunt, with an admittance inverter on each side looks like a series-type resonator connected in series. Table I gives the equations needed for relating the parameters of the circuit in Fig. 2(b) to that in 2(a). The frequencies ω_1 and ω_2 are the band-pass cut-off frequencies corresponding to the low-pass cut-off frequency ω_1' for the prototype. Observe that the band-pass filter designs are defined in terms of the external Q's, $(Q_e)_1$ and $(Q_e)_n$ for the end resonators, and the coupling coefficients $k_{j,j+1}$ between resonators. The resonators are all resonant at the same frequency ω_0, and their susceptance slope is characterized by a susceptance slope parameter defined by

$$b = \frac{\omega_0}{2} \left.\frac{dB}{d\omega}\right|_{\omega = \omega_0} \qquad (1)$$

where $dB/d\omega$ is the slope of the susceptance characteristic at the resonant frequency ω_0. In Fig. 2(c) the x_j are the reactance slope parameters of the series-type resonators, and are defined in analogous fashion. For a given transmission characteristic, aside from the fact that all resonators must resonate at the same frequency, the choice of resonator designs is arbitrary provided appropriate inverters and terminations are used as indicated in Eqs. (d) and (e) of Table I. The dual relations in Eqs. (f) and (g) hold for the circuit in Fig. 2(c).

Coupling Through Reflecting Arrays

It is known that filters can be formed by structures of the form in Fig. 3(a).[6,7,1] The rectangles marked $N_{j,j+1}$ are reflecting arrays each having $N_{j,j+1}$ reflecting elements modelled as in Figs. 1(b) and 4(a). The arrays are resonant at the frequency for which the line sections are a quarter-wavelength long. It can be seen that for resonance the spacing between arrays must be such that the leading edges E of the array models will be a multiple m_{sj} of half-wavelengths apart as indicated in Fig. 1(b). Surface-wave energy is incident form the left in Fig. 3(a) and the structure comprises a four-resonator filter with the regions of the different resonators indicated by the numbers below. Various treatments of such structures exist,[6,7,1] but herein it will be shown how such structures can be designed with great ease and flexibility by use of the viewpoint in Fig. 2 and Table I.

It can be shown[9] that an array having $N_{j,j+1}$ reflecting elements can be modelled by one or the other of the equivalent circuits in Fig. 4(b), (c) where the resonator slope parameters are

$$\left.\begin{matrix} b_{j,j+1} \\ \text{or} \\ x_{j,j+1} \end{matrix}\right\} = \frac{\pi\left(1 - \frac{1}{u^{2N_{j,j+1}}}\right)\left[\left(1 + \frac{1}{u}\right) - \left(\frac{(1+u)}{u^{2N_{j,j+1}}}\right)\right]}{4\left(u - \frac{1}{u}\right)}, \qquad (2)$$

and the inverter parameters are

$$\left.\begin{matrix} J_{j,j+1} \\ \text{or} \\ K_{j,j+1} \end{matrix}\right\} = \frac{1}{u^{N_{j,j+1}}}. \qquad (3)$$

In the present application we are free to define the free-surface surface-wave impedance arbitrarily, and for

†This research was supported by NSF Grant ENG 76-00195.

convenience we chose $Z_0 = 1/Y_0 = 1$, which is assumed in (2) and (3). If $r > 1$ (as in the case of open-circuited metal strip arrays,[8,4] and waffle-iron metal arrays[10]) $u = r$ and the circuit in Fig. 4(b) applies. From Fig. 4(b) it is seen that for the case of $r > 1$ an array structure as in Fig. 3(a) can be modelled by a structure as in Fig. 2(b), where the total resonator slope parameter due to adjacent arrays $N_{j-1,j}$ and $N_{j,j+1}$ and their intervening spacing m_{sj} is given by

$$b_j = b_{j-1,j} + \frac{m_{sj}\pi}{2} + b_{j,j+1} \quad , \tag{4}$$

and analogously for the dual case of x_j if $r < 1$.

For Fig. 3(a) the correct loading conductances G_{L1} and G_{Ln} are given by

$$G_{L1} = J_{01}^2/Y_0 \quad , \quad G_{Ln} = J_{n,n+1}^2/Y_0 \tag{5}$$

where J_{01} and $J_{n,n+1}$ are the inverter parameters associated with arrays N_{01} and $N_{n,n+1}$ (here $n = 4$), and where herein $Y_0 = 1$. In the case of the terminating arrays N_{01} and N_{45}, the resonators with slope parameters b_{01} and b_{45} at the ends of the structure can be ignored in the design process because those resonators are terminated by the free-surface admittance Y_0 and have a selectivity which is extremely broad compared with that of the rest of the structure. Since the value of $N_{j,j+1}$ fixes both $J_{j,j+1}$ and $b_{j,j+1}$, it is found that iterative use of Eqs. (2) to (5), and (d) and (e) of Table I gives good results.[9] This procedure is found to converge very rapidly and, within limits, the values of the m_{sj} can be arbitrary integers.

At A in Table II is shown the design parameters for a filter of the form in Fig. 3(a) designed from a low-pass Chebyshev prototype with 0.10-dB ripple, for a fractional bandwidth of $w = .0015$. The arrays were assumed to have $r = 1.011$ as for a typical waffle-iron structure[10] on YZ, $LiNbO_3$. The solid lines in Fig. 5 show the computed response for this design, and it is seen that the passband conforms very closely to the design specifications. However, as expected, the stopband gives out not far from the passband because the bandwidth for high reflection from the arrays is very limited.

Electric Coupling Using Transducers

In practical situations it is necessary to use transducers for going from an electrical source into the surface-wave filter and from the filter to the electrical load. Fig. 3(b) shows a modified design including transducers with $n_1 = n_4 = 11$ fingers. In this case the outer arrays N_{R1} and N_{R4} are purely for the purpose of reflecting energy rather than for coupling to external acoustic terminations. Thus the number of reflecting elements in these arrays is greatly increased (in this case to 300). The mutual coupling arrays were redesigned to accomodate the change in resonator slope parameters due to the changed end arrays and due to changing $m_{s1} = m_{s4}$ from 15 to 12. The transducers were designed using methods similar to those described in Ref. 3.* An electromechanical coupling coefficient of $k_c = 0.2$ as for $LiNbO_3$ was assumed for the transducers along with a center frequency of 30 MHz and transducer capacitances of 26.5 pf. The final design parameters are summarized at B in Table II. Note that the m_{s1} and m_{s4} values are no longer integers since the transducers require a compensating tuning correction.[3,9] The computed response for this design is indicated by the dashed lines in Fig. 5. Note that the pass-band region is much the same as for the first design except for some loss due to leakage out arrays N_{R1} and N_{R4}, and that the stop-band attenuation has been enhanced somewhat.

In order to further enhance the minimum attenuation level in the stopband, electric transducer coupling between resonators 2 and 3 was introduced as shown in Fig. 3(c), again using design procedures such as those in Ref. 3 and herein.[9] For simplicity, transducers n_2 and n_3 were also designed to have 11 fingers, which gave excessive coupling, which in turn was reduced by inclusion of the decoupling capacitor C_{23}. The parameters for this design are summarized at C in Table II. The computed response for this design is shown by the solid lines in Fig. 6. In this case the minimum stopband attenuation is around 30 dB. This would be higher if the bandwidth of the filter were narrower or if additional transducer couplings were used.

Multistrip Coupling of Resonators

It is known that multistrip couplings can be used for coupling of surface-wave resonators.[11,12,13] That this should work can be seen from the fact that the signal coupled out the adjacent track of a multistrip coupler has a 90° phase shift with respect to the signal out the straight-through track. Thus a multistrip coupler will have inverting properties such that it can be used as an admittance or impedance inverter. Also, its directional coupling properties provide an alternate means for enhancing attenuation in the stopband region where the arrays are not reflecting. Let us consider the case of the use of a multistrip coupler for coupling between resonators 2 and 3 in Fig. 3(c). It can be shown[9] that the equivalent admittance inverter $J_{j,j+1}$ for a multistrip coupler which couples a fraction c^2 of the incident power into the adjacent track is given by

$$J_{j,j+1} = \frac{c}{\sqrt{1-c^2}} \tag{6}$$

where $c = \sqrt{P_c/P_{inc}}$, P_c is the power transferred to the adjacent track, P_{inc} is incident power in the initial track, and where $Y_0 = 1$ was assumed. In the case of the example in Fig. 3(c) an admittance inverter with admittance $J_{23} = .154$ is required in order to give proper coupling between the given resonators. Solving Eq. (6) for c^2 gives $c^2 = .0231$ (i.e., 16.3 dB coupling is required). This calls for a multistrip coupler with

*The two equations following (17) in Ref. 3 should have a minus sign appended before the parameters G_{Aj}, G_{Bj}, and G_{Ap}.

11 strips when using $LiNbO_3$.[14] The final design would be of the form in Fig. 3(c) but with transducers n_2 and n_3 replaced by a multistrip coupler. Note that when the arrays are not reflecting the energy incident from transducer n_1 will be directed by the multistrip coupler away from transducer n_4. In this way transducers n_1 and n_4 tend to be isolated when the arrays are not reflecting. However, since at most frequencies arrays have some small amount of reflection outside of their stop-band region, some energy would still be scattered to the output transducer n_4. Using analysis procedures described in Ref. 9 the response for the circuit in Fig. 3(c) using multistrip coupling between resonators 2 and 3 was computed, and the result is shown by the dashed lines in Fig. 6. At least for this example the stop-band attenuation is somewhat inferior using a multistrip coupler than when using transducer coupling.

Conclusions

It is seen that SAW resonator filters with any of a variety of coupling mechanisms can be conveniently designed using the point of view of Fig. 2 and Table I. Our previous measured results indicate that array coupling as in Fig. 3(a) has less loss than transducer coupling (even if loss out the ends of the arrays such as N_{R1} and N_{R4} in Fig. 3(b) is negligible).[10] However, since array coupling gives poor stop-band attenuation some transducer couplings or multistrip couplings will be necessary in most practical cases. Thus structures such as that in Fig. 3(c) may provide a useful compromise. In the examples of Fig. 6 the replacing of transducer coupling between resonators 2 and 3 with multistrip coupling gave somewhat inferior stop-band performance. Another possible difficulty with the use of multistrip coupling is that some energy would be lost in the space between resonators 2 and 3.

References

1. Staples, E. J., and Smythe, R. C., Proc. 1976 Freq. Control Symposium.

2. Bell, D. J., Jr. and Li, R. C. M., Proc. IEEE, Vol. 64, pp. 711-721, May 1976.

3. Matthaei, G. L., Barman, F., Savage, E. B., and O'Shaughnessy, B. P., 1975 Ultrasonics Symposium Proc., pp. 284-289.

4. Matthaei, G. L., Barman, F., Savage, E. B., Electronics Letters, Vol. 21, pp. 556-557, 14 Oct. 1976.

5. Matthaei, G. L., Young, L., and Jones, E. M. T., Microwave Filters, Impedance-Matching Networks and Coupling Structures, McGraw-Hill, N.Y., 1964.

6. Li, R. C. M., Alusow, J. A., and Williamson, R. C., Proc. 1975 Freq. Control Symposium, pp. 167- .

7. Cross, P. S., Schmidt, R. V., and Haus, H. A., 1976 Ultrasonics Symposium Proc., pp. 277-280.

8. Matthaei, G. L., O'Shaughnessy, B. P., and Barman, F., IEEE Trans. SU, Vol. SU-23, pp. 99-107, March 1976.

9. Full-length version of this paper now in preparation.

10. Matthaei, G. L. and Barman, F., 1976 Ultrasonics Symposium Proc., pp. 415-418.

11. Hartmann, C. S. and Rosenfeld, R. C., U.S. Patent No. 3,886,504, May 27, 1975.

12. Redwood, M., Topolevsky, R. V., Mitchell, R. F., and Palfreeman, J. S., Electron. Lett., Vol. 11, pp. 253-254, 1975.

13. Rosenberg, R. L. and Coldren, L. A., 1976 Ultrasonics Symp. Proc., pp. 281-286.

14. Marshall, F. G., Newton, C. O., and Paige, E. G. S., IEEE Trans. SU, Vol. SU-20, pp. 124-143, 1973.

Table I

Band-pass filter parameters from low-pass prototype in Fig. 2(a):

$$\omega_0 = \frac{\omega_2 + \omega_1}{2} \quad , \quad w = \frac{\omega_2 - \omega_1}{\omega_0} \tag{a}$$

$$\left(Q_e\right)_1 = \frac{g_0 g_1 \omega_1'}{w} \quad , \quad \left(Q_e\right)_n = \frac{\omega_1' g_n g_{n+1}}{w} \tag{b}$$

$$k_{j,j+1}\Big|_{j=1 \text{ to } n-1} = \frac{w}{\omega_1' \sqrt{g_j g_{j+1}}} = \text{coupling coefficient} \tag{c}$$

For structure in Fig. 2(b):

$$G_{L1} = \frac{b_1}{\left(Q_e\right)_1} \quad , \quad G_{Ln} = \frac{b_n}{\left(Q_e\right)_n} \tag{d}$$

$$J_{j,j+1}\Big|_{j=1 \text{ to } n-1} = k_{j,j+1}\sqrt{b_j b_{j+1}} \text{ mhos} \tag{e}$$

For structure in Fig. 2(c):

$$R_{L1} = \frac{x_1}{\left(Q_e\right)_1} \quad , \quad R_{Ln} = \frac{x_n}{\left(Q_e\right)_n} \tag{f}$$

$$K_{j,j+1}\Big|_{j=1 \text{ to } n-1} = k_{j,j+1}\sqrt{x_j x_{j+1}} \text{ ohms} \tag{g}$$

Table II

Design in Fig. 3(a):

$r = 1.011$, $N_{01} = N_{45} = 77$, $N_{12} = N_{34} = 161$, $N_{23} = 183$, $m_{s1} = m_{s4} = 15.0000$, $m_{s2} = m_{s3} = 1.0000$.

Design in Fig. 3(b):

$r = 1.011$, $N_{R1} = N_{R4} = 300$, $N_{12} = N_{34} = 155$, $N_{23} = 183$, $m_{s1} = m_{s4} = 12.0361$, $m_{s2} = m_{s3} = 1.0000$, $n_1 = n_4 = 11$, $C_T = 26.5$ pf, $k_c = 0.2$, $R_A = R_B = 107.2$, $f_0 = 30$ MHz.

Design in Fig. 3(c):

$r = 1.011$, $N_{R1} = N_{R2} = N_{R3} = N_{R4} = 400$, $N_{12} = N_{34} = 150$, $m_{s1} = m_{s4} = 12.0358$, $m_{s2} = m_{s3} = 12.0490$, $n_1 = n_2 = n_3 = n_4 = 11$, $C_T = 26.5$ pf, $k_c = .2$, $R_A = R_B = 106.6$, $C_{23} = 34.6$ pf, $f_0 = 30$ MHz.

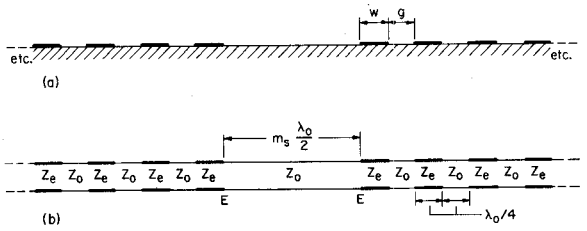

Fig. 1. (a) A surface-wave resonator. (b) Its transmission-line equivalent.

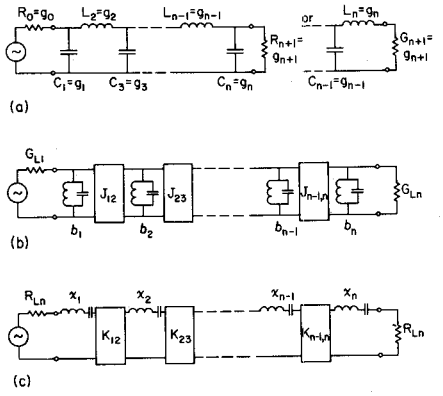

Fig. 2. (a) A low-pass prototype filter. (b), (c) Corresponding band-pass filters.

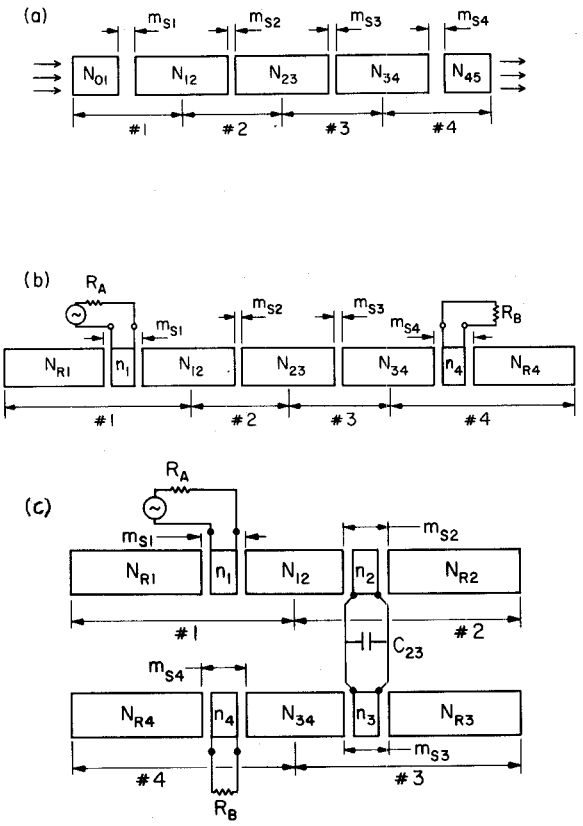

Fig. 3. Three, four-resonator, filters using surface-wave resonators with various coupling arrangements.

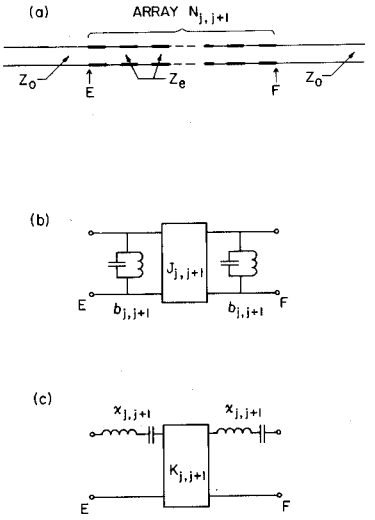

Fig. 4. (a) Transmission-line equivalent circuit for a surface-wave array. (b), (c) Simplified array equivalent circuits valid at or near resonance when $r > 1$ and $r < 1$, respectively.

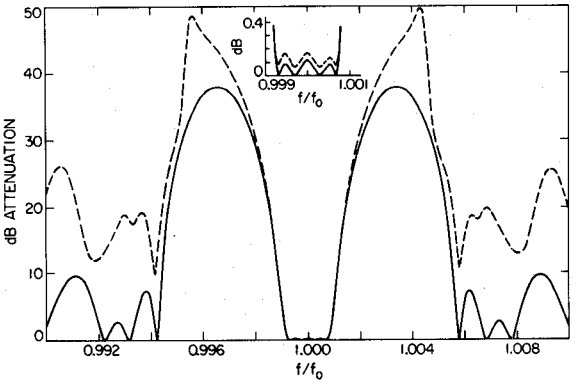

Fig. 5. The solid lines show the computed response of the example of Fig. 3(a), and the dashed lines show the corresponding response for the example of Fig. 3(b).

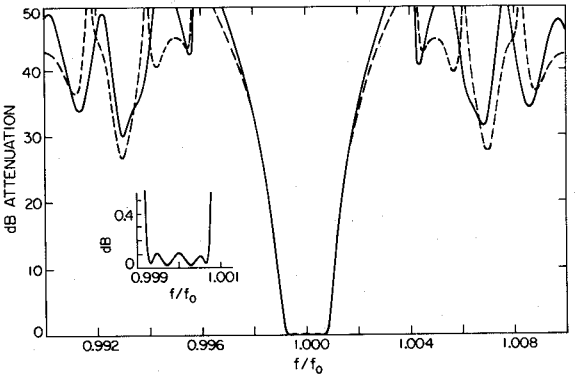

Fig. 6. The solid line shows the computed response for the example of Fig. 3(c), while the dashed lines shows the corresponding response using multistrip coupling between resonators 2 and 3.